precipitate (0.35 g, 0.21 mmol). Anal. Calcd for $C_{79}H_{65}BF_7P_5Pd_3S$: C, 57.0; H, 3.9. Found: C, 57.2; H, 4.2. Molar conductance was 75 Ω^{-1} cm^2.

$[Pd_3(SCF_3)(PPh_2)_2(PEt_3)_3][BF_4]$. This complex was similarly prepared in similar yield from $[Pd_3Cl(PPh_2)_2(PEt_3)_3][BF_4]$. Anal. Calcd for $C_{43}H_{65}BF_7P_5Pd_3S$: C, 41.9; H, 5.3. Found: C, 41.3; H, 5.4. Molar conductance was 80 Ω^{-1} cm^2.

Acknowledgment. We thank the National Research Council of Canada and the University of Victoria for research grants, Dr. A. Pidcock for access to ^{31}P NMR facilities at the University of Sussex, and Dr. D. R. Coulson for providing an infrared spectrum of his cluster complex.

Registry No. $[Pd_3Cl(PPh_2)_2(PPh_3)_3][BF_4]$, 65916-07-6; $[Pd_3Cl(PPh_2)_2(PEt_3)_3][BF_4]$, 65916-06-5; $[Pd_3Cl(PPh_2)_2(PMe_2Ph)_3][BF_4]$, 65916-05-4; $[Pd_3Cl(PPh_2)_2(PPh_3)_3][Cl]$, 65859-21-4; $[Pd_3Br(PPh_2)_2(PPh_3)_3][Br]$, 65859-20-3; $[Pd_3I(PPh_2)_2(PPh_3)_3][I]$, 65859-19-0; $[Pd_3Br(PPh_2)_2(PEt_3)_3][BF_4]$, 65916-04-3; $[Pd_3(SCF_3)(PPh_2)_2(PPh_3)_3][BF_4]$, 65916-03-2; $[Pd_3(SCF_3)(PPh_2)_2(PEt_3)_3][BF_4]$, 65916-02-1; $[PdCl(PPh_3)_3][BF_4]$, 34772-26-4.

References and Notes

(1) R. B. King, *Prog. Inorg. Chem.*, **15**, 287 (1972).
(2) R. Ugo, S. Cenini, M. F. Pilbrow, B. Deibl, and G. Schneider, *Inorg. Chim. Acta*, **18**, 113 (1976), and references therein.
(3) R. G. Vranka, L. F. Dahl, P. Chini, and J. Chatt, *J. Am. Chem. Soc.*, **91**, 1574 (1969).
(4) A. Albinati, G. Carturan, and A. Musco, *Inorg. Chim. Acta*, **16**, L3 (1976).
(5) D. C. Moody and R. R. Ryan, *Inorg. Chem.*, **16**, 1052 (1977).
(6) M. Green, J. A. Howard, J. L. Spencer, and F. G. A. Stone, *J. Chem. Soc., Chem. Commun.*, 3 (1975).
(7) J. C. Calabrese, L. F. Dahl, P. Chini, G. Longini, and S. Martinengo, *J. Am. Chem. Soc.*, **96**, 2614 (1974).
(8) N. J. Taylor, P. C. Chieh, and A. J. Carty, *J. Chem. Soc., Chem. Commun.* 448 (1975).
(9) T. Yoshida and S. Otsuka, *J. Am. Chem. Soc.*, **99**, 2134 (1977).
(10) M. Hidai, M. Kokura, and Y. Uchida, *J. Organomet. Chem.*, **52**, 431 (1973).
(11) F. Klanberg and E. L. Muetterties, *J. Am. Chem. Soc.*, **90**, 3296 (1968).
(12) S. Otsuka, Y. Tatsumo, M. Miki, T. Aoki, M. Matsumoto, H. Yoshida, and K. Nakatsu, *J. Chem. Soc., Chem. Commun.*, 445 (1973).
(13) D. R. Coulson, *Chem. Commun.*, 1530 (1968).
(14) G. W. Bushnell, K. R. Dixon, P. M. Moroney, A. D. Rattray, and Ch'eng Wan, *J. Chem. Soc., Chem. Commun.*, 709 (1977).
(15) K. R. Dixon, K. C. Moss, and M. A. R. Smith, *J. Chem. Soc., Dalton Trans.* 1528 (1973).
(16) The products always contained ~1 mmol of $POPh_3$ for each mmol of cluster but the significance of this is not clear. Preliminary purification of the tetrahydrofuran (potassium–benzophenone) should exclude water and organic carbonyl species as sources of the oxygen and oxidation of PPh_3 does not occur during product workup since $POPh_3$ can be sublimed directly from the reaction products in vacuo. In view of the ease of Lewis acid catalyzed cleavage of ethers and the known ability of PPh_3 to deoxygenate many organic compounds,[17] it is possible that tetrahydrofuran itself is the source of oxygen. However, some cluster formation was still observed in reactions conducted in benzene. An anonymous reviewer suggested that the reaction may be $3[PdCl(PPh_3)_3]^+ \rightarrow [Pd_3Cl(PPh_2)_2(PPh_3)_3]^+ + 2[PPh_4]^+ + PPh_3 + PCl_2Ph_3$. The $POPh_3$ could then arise by hydrolysis of PCl_2Ph_3, possibly by moisture brought in with the reagent palladium salt.
(17) L. F. Fieser and M. Fieser, "Reagents for Organic Synthesis", Wiley-Interscience, New York, N.Y., 1967, pp 1242–1249; R. C. Fuson, "Reactions of Organic Compounds", Wiley, New York, N.Y., 1962, pp 161–164.
(18) W. J. Geary, *Coord. Chem. Rev.*, **7**, 81 (1971).
(19) K. R. Dixon, unpublished observations.
(20) J. A. Pople, W. G. Schneider, and H. J. Bernstein, "High Resolution Nuclear Magnetic Resonance", McGraw-Hill, New York, N.Y., 1959, pp 123–128.
(21) For example, if we approximate the two triethylphosphine groups (CH_3–CH_2–P---P–CH_2–CH_3) as an $A_3X_2MM'X_2'A_3'$ spin system, then the methyl resonance changes from a doublet (J_{AM}) of triplets (J_{AX}) to an overlapping triplet ($J_{apparent} = {}^1/_2(J_{AM} + J_{AM'})$) of triplets ($J_{AX}$) as $J_{MM'}$ increases in magnitude.[23] Clearly, the analysis is not rigorous in our molecules since other phosphorus atoms are present but it does provide an order of magnitude for the P–P coupling ($J_{BB'}$).
(22) J. F. Nixon and A. Pidcock, *Annu. Rev. NMR Spectrosc.*, **2**, 380 (1969).
(23) K. R. Dixon, K. C. Moss, and M. A. R. Smith, *Can. J. Chem.*, **52**, 692 (1974), and references therein.
(24) K. R. Dixon and D. J. Hawke, *Can. J. Chem.*, **49**, 3252 (1971).
(25) Present work and K. O'Dell, D. Phil. Thesis, University of Sussex, 1976.
(26) R. B. Johannesen, J. A. Ferreti, and R. K. Harris, *J. Magn. Reson.*, **3**, 84 (1970).
(27) J. D. Swalen in "Computer Programs for Chemistry", Vol. I, D. F. Detar, Ed., W. A. Benjamin, New York, N.Y., 1968.
(28) R. G. Hayter, *J. Am. Chem. Soc.*, **84**, 3046 (1962).
(29) Some reactions were stopped after a shorter time if decomposition to metallic Pd was excessive.
(30) G. Wittig and E. Benz, *Chem. Ber.*, **92**, 1999 (1959).
(31) J. W. Daasch and D. C. Smith, *Anal. Chem.*, **23**, 853 (1951).

Contribution from the Department of Chemical Engineering, Stanford University, Stanford, California 94305

Ligand and Cluster Effects in the Decomposition of Formic Acid on Cu/Ni (110) Single-Crystal Surfaces

D. H. S. YING and ROBERT J. MADIX*

Received August 29, 1977

The decomposition of formic acid on single-crystal copper–nickel alloy surfaces of (110) orientation was studied to elucidate the relative importance of surface composition on the decomposition selectivity and activity. The CO:CO_2 product ratio decreased steeply with increasing copper surface content. This pronounced effect was due to the requirement of a small cluster of four nickel atoms on the surface to form the CO-producing intermediate, adsorbed formic anhydride. The activation energy for decomposition of the anhydride increased by 2 kcal/mol over the Cu/Ni surface composition range studied, reflecting a weak ligand effect on the surface reactivity.

Introduction

Recent studies of the flash decomposition of formic acid on single-crystal surfaces of nickel and copper[1-4] have shown that the selectivity ratio CO:CO_2 varies from unity on Ni(110) to zero on Cu(110). The selectivity is governed by the degree of admixture of two different reaction pathways involving adsorbed formic anhydride or formate, respectively. Whereas on Ni(110) the flash decomposition of formic acid proceeded solely via the anhydride intermediate, on Cu(110) the formate intermediate was formed alone. This sharp difference in the chemical behavior of these two surfaces provided an interesting opportunity for studying the relative importance of ligand and cluster effects in the surface reactivity of alloys, as discussed below.

Metal alloys have long been a subject of interest in catalysis.[5-11] Major effects on selectivity and activity have been noted, and these effects have been ascribed traditionally to "electronic" and "geometric" effects. Recent photoemission work on the Ni/Cu alloy system by Spicer et al.[12,13] utilizing short electron escape depths, illustrated that the surface electronic properties of the alloy were simply the superpositions of the surface electronic properties of every *separate* metal.

0020-1669/78/1317-1103$01.00/0

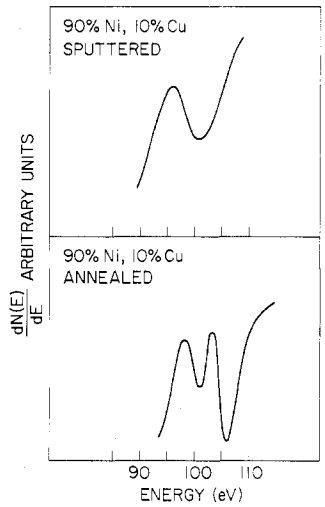

Figure 1. Auger spectra from the $M_1M_{4,5}M_{4,5}$ transition for the Cu/Ni alloy.

This result illustrated that the atoms of copper and nickel retained their local atomic identity even though they formed a *homogeneous* alloy system. It would be expected, therefore, that a study of a strongly selective reaction on a single-crystal Cu/Ni alloy would yield information regarding the cluster size and shape necessary to form reaction intermediates.

The customary electronic and the geometric effects are not well-defined, and it is more appropriate to interpret the catalytic activity of alloys in terms of ligand effects and the requirement of clusters of active metal atoms for adsorption or product formation. Ligand effects denote here the change of the adsorption strength or activation energy for a foreign species bound to a metal atom A or group of A atoms when some or all of its neighboring atoms are replaced by a different type of atom B. The term cluster requirement is reserved for the need of a cluster of n atoms A for the chemisorption of a molecular species or for the formation of a particular surface intermediate. This group of n atoms A is called a "homogeneous" cluster. In the interpretation of the surface-reactive behavior of alloys, cluster requirements have not received as much attention as the ligand effect. In the present study the importance of the cluster requirement in the surface reactivity of the Ni/Cu alloy system as well as the ligand effect was demonstrated.

Experimental Section

The Ni/Cu alloy single crystal employed in the present study was (110) oriented with a bulk composition of 90% Ni and 10% Cu. The surface of the sample was cleaned by Ar ion bombardment at room temperature and subsequently annealed at a higher temperature and quenched back to room temperature. The surface composition of the sample was characterized by Auger electron spectroscopy. Figure 1 shows the Auger spectra from the $M_1M_{4,5}M_{4,5}$ transition at roughly 100 eV for the sputtered and the annealed alloy surfaces. Surface copper was preferentially sputtered as shown in Figure 1, the spectrum exhibiting a single nickel peak indicating 100% Ni on the alloy surface. In general the alloy surface was copper enriched after annealing because of segregation of the copper atoms. This was in agreement with the theoretical prediction from the regular solution model developed by Williams et al.,[14,15] suggesting that the component of a binary alloy having the lower heat of sublimation would segregate to the surface. This surface enrichment with copper was also predicted by a model developed recently by Burton et al.[16] using the bulk-phase equilibrium diagram. Both nickel and copper peaks were observed in the Auger spectrum of the alloy after sputtering and annealing at 650 °C as shown in Figure 1. This Auger spectrum was doubly integrated to obtain the Auger intensities of nickel and copper which were used directly to calculate the relative surface concentration of the alloy. The first integration provided the total $N(E)$ signal which was then separated into a Ni component and a Cu component according to the energy positions of the elemental standard. These components were integrated separately to obtain their Auger intensities. Backscattering can be a significant factor in the quantitative determination of the surface composition of alloys by AES. Fortunately, the atomic numbers of Ni and Cu are so close (28 and 29, respectively) that backscattering did not affect the AES-determined Ni/Cu alloy surface composition. The short electron escape depth[17] at this energy range and the mode of energy analysis also ensured that only the first one or two atomic layers were examined. Therefore, the "Auger-measured" surface composition represented an exponentially averaged concentration within one or two atomic layers. By taking advantage of an extremely slow bulk-diffusion process,[18,19] the amount of copper segregation could be controlled by varying the annealing temperature. Hence, different surface compositions were prepared by choosing appropriate annealing temperatures as shown in Table I. The results were in agreement with those reported previously by Spicer et al.[12,20,21] using the same technique.

Table I. The Annealing Temperatures and the Resulting Surface Composition of the Ni/Cu(110) Alloy

ANNEALING TEMPERATURE °K	SURFACE COMPOSITION	
	% Ni	% Cu
699	87	13
770	77	23
805	68	32
829	61	39
852	54	46
875	46	54
899	37	63

The catalytic decomposition of formic acid was studied by means of flash-desorption spectroscopy. The experiments were carried out in a stainless steel ultra-high-vacuum reaction chamber maintained at the range of 10^{-10} Torr by means of a noble vac-ion pump and a titanium sublimation pump.[22] After the desired surface composition was obtained, the sample was exposed to the previously purified formic acid vapor[22] through a stainless steel dosing needle. The sample was then heated linearly with time by radiation from a tungsten filament to decompose the preadsorbed species, and the partial pressure rise of the gaseous products was recorded by a mass spectrometer as a function of the sample temperature which was measured by a chromel–alumel thermocouple spark welded at the corner of the sample. The pumping speed of the system was sufficiently high that the mass spectrometric signals were directly proportional to the desorption rates of the respective products.[23] The distribution of the decomposition products yielded information about the reaction intermediates and the rate-governing reaction step. In addition, the kinetic rate constants for the decomposition were obtained from the profile of the desorption spectrum and the temperature at maximum desorption rate. No detectable change in the surface composition of the alloy due to the decomposition reaction was found, as checked by AES examination of the alloy surface composition at the beginning and end of the experiments.

A special experiment called "interrupted" flash was performed as follows. After formic acid was dosed on the alloy surface, the sample was heated to a temperature high enough to partially desorb one of the products, i.e., higher than the temperature where the product started to desorb but too low to effect complete desorption. The sample was quickly cooled back to the initial adsorption temperature and then heated up again to obtain a complete flash-desorption spectrum. This resulting product desorption spectrum was called the "interrupted" spectrum. This experiment was sometimes repeated with successively higher "interrupted" temperature to obtain a series of "interrupted"

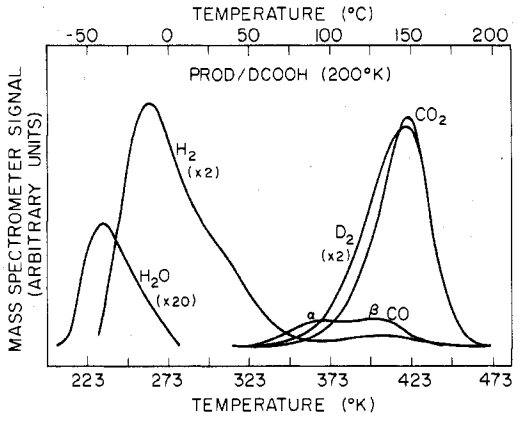

Figure 2. Product distribution following the adsorption of DCOOH to saturation on an alloy with a surface composition of 37% Ni/63% Cu at 200 K. Heating rate was 12 K/s.

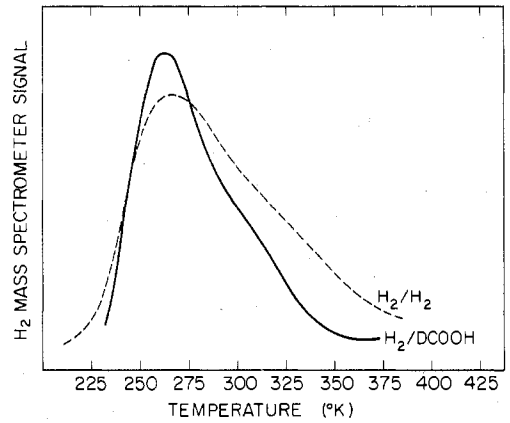

Figure 3. Comparison of the H_2/DCOOH spectrum with the H_2/H_2 desorption spectrum. The alloy surface composition was 37% Ni/63% Cu. The H_2/H_2 desorption spectrum was obtained from ref 20.

spectra. A shorthand notation was employed to identify the origin of the desorbing gas as

$$x(\alpha)/y$$

where x was the desorbing gas observed, α was the binding state of the gas x, and y was the preadsorbed gas. For example, CO(α)/DCOOH refers to the α state of the CO product following the adsorption of DCOOH.

Results and Discussion

Figure 2 shows the product distribution following the adsorption of deuterated formic acid (DCOOH) at 200 K on an alloy with a surface composition of *37% Ni/63% Cu*. The major decomposition products observed were CO_2, D_2, and H_2. Small amounts of H_2O and CO products were also present. The total CO signal amounted to one-tenth of the CO_2 product. The H_2 product peak was located below room temperature at 258 K as shown in Figure 2. A comparison of this H_2 product spectrum with the H_2/H_2 desorption spectrum indicated that the H_2/DCOOH product was desorption limited as shown in Figure 3. There was no hydrogen-binding state corresponding to the D_2/DCOOH product peak, however, suggesting that the D_2 product was decomposition limited. Furthermore no CO_2-binding state was observed at all on the alloy surface; the CO_2 product would desorb immediately once it was formed. Hence, its formation was also decomposition limited.

When the adsorption temperature was increased from 200 to 300 K, CO_2, D_2, and CO were the only products observed. The peak positions of these observed products were not affected by the change of the adsorption temperature from 200 to 300 K which is further evidence against surface reconstruction with

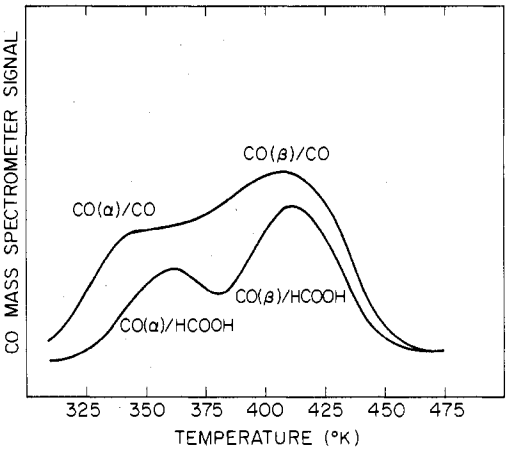

Figure 4. Comparison of the CO/HCOOH spectrum with the CO/CO desorption spectrum. The alloy surface composition was 61% Ni/39% Cu. The adsorption temperature was 399 K.

adsorption. As shown in Figure 2, the two CO product peaks were not distinct enough to allow the comparison with the CO/CO desorption spectrum. Nevertheless the presence of the D_2/DCOOH product and the high CO_2:CO selectivity ratio (10:1) suggested that the major surface intermediate on this alloy surface was an adsorbed formate, DCOO(a).

As the surface nickel concentration was increased, the selectivity ratio CO:CO_2 increased, and the peak positions of the decomposition products shifted—though the same products were observed. In addition, the peak positions of the two CO product peaks became more distinct, allowing comparison with the CO/CO desorption spectrum. Figure 4 shows the CO/HCOOH product and CO/CO[24] desorption spectra on an alloy with a surface composition of 61% Ni/39% Cu. The matching of the β states indicated that the CO(β)/HCOOH product was desorption limited. The CO(α)/HCOOH peak was at least 15 K higher than the CO(α)/CO peak. This difference indicated that the CO(α)/HCOOH peak was not desorption limited and that the CO(α) product was evolved directly into the gas phase from a decomposition step.

The reaction mechanism for the formic acid decomposition on the Ni/Cu (110) alloy was as follows: dissociative adsorption steps

$$DCOOH(g) \rightarrow DCOO(a) + H(a) \quad (1)$$

$$2DCOOH(a) \rightarrow D(O)COC(O)D(a) + H_2O(a) \quad (2)$$

$$2H(a) \rightarrow H_2(g) \quad (3)$$

$$H_2O(a) \rightarrow H_2O(g) \quad (4)$$

and decomposition steps

$$D(O)COC(O)D(a) \rightarrow CO_2(g) + xCO(g) + (1-x)CO(a) + 2D(a) \quad (5)$$

$$DCOO(a) \rightarrow CO_2(g) + D(a) \quad (6)$$

$$2D(a) \rightarrow D_2(g) \quad (7)$$

$$CO(a) \rightarrow CO(g) \quad (8)$$

The first two steps occurring were adsorption of the parent molecule (DCOOH) to form two different adsorbed surface intermediates: DCOO(a) and formic anhydride. The H atoms recombined to form the H_2 molecule which desorbed from the surface. Steps 3 and 4 show the desorption of the H_2 and H_2O products. Since these two products desorbed below 300 K, they were not detected in the room-temperature adsorption study. Steps 5 and 6 represent the decomposition of the two different surface intermediates giving rise to the three major products (CO_2, D_2, and CO). The CO_2 product was formed from the decomposition of both intermediates. The recombination of the hydrogen atoms shown in step 7 was a relatively fast process, so that the decomposition steps limited the rate

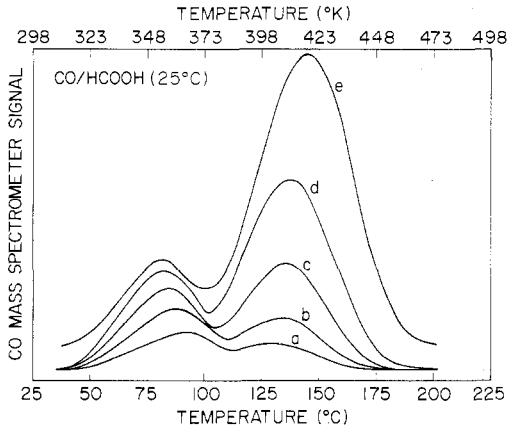

Figure 5. CO product flash-desorption spectra as a function of surface composition of the alloy: curve a, 37% Ni/63% Cu; curve b, 46% Ni/54% Cu; curve c, 54% Ni/46% Cu; curve d, 61% Ni/39% Cu; curve e, 68% Ni/32% Cu. The heating rate was 13 K/s.

of the D_2/DCOOH formation. The direct gaseous evolution of the CO product shown in step 5 gave rise to the CO(α) product peak. Hence, the kinetic parameters for the formation of this CO(α) product peak reflected those for the decomposition of the formic anhydride intermediate on the alloys. Finally, the desorption-limited CO(β) product is shown in step 8. It is important to point out that since the CO formation was totally suppressed on a clean Cu(110) surface,[4] it is reasonable to believe the formic anhydride to be adsorbed only to the surface nickel atoms in the alloy.

Three interesting features were observed from the CO product spectrum as the alloy surface nickel concentration was decreased. First of all, the CO(β) product peak shifted to lower temperatures as shown in Figure 5. Since the CO(β) peak was desorption limited, the shift of the CO(β) peak was ascribed to the ligand effect of copper to the surface nickel atoms of the alloy.[20,21] When copper was added to nickel, the adsorption strength of the CO molecules was lowered. Hence, the activation energy required for the CO desorption was lowered, resulting in a shift of the CO(β) peak to a lower temperature. A decrease of 3 kcal/mol was estimated from the total shift of the CO(β) peak with the assumption of a constant preexponential factor.

In opposition to the CO(β) peak, the CO(α) peak moved to higher temperatures as the nickel surface concentration was reduced. This shift was also ascribed to the ligand effect of copper on the surface nickel atoms. If it was assumed that the formic anhydride intermediate was adsorbed on the surface nickel sites through the two oxygen atoms and its adsorption strength was lowered with the addition of copper atoms in a similar manner as the CO molecules, then extra energy was required to rupture one of the two C–O bonds. Hence, the formic anhydride decomposition energy increased with the addition of copper to nickel, shifting the CO(α) peak to a higher temperature corresponding to an increase of roughly 2 kcal/mol in activation energy with the assumption of a constant preexponential factor.

Lastly, there was a substantial decrease in the amount of CO formed as the nickel surface concentration was lowered, suggesting the necessity of a cluster of more than one nickel atom for CO formation on the alloy. Statistically, on a substitutional alloy surface with nickel concentration X_{Ni}, the probability of the existence of clusters of n nickel atoms is proportional to X_{Ni}^n. This conclusion is based on a statistical calculation for a model of random alloying. Recently, Spicer et al.[12,13] examined the surface clustering problem and concluded that preferential surface clustering was negligible on the Ni/Cu (110) alloy sample. This conclusion was based on

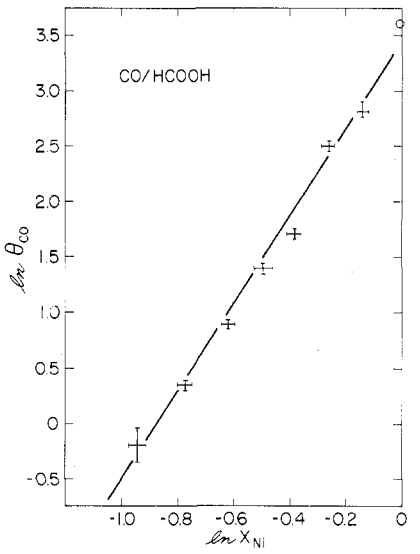

Figure 6. ln–ln plot of CO/HCOOH product at saturation coverage vs. the nickel surface fraction: θ_{CO}, CO product at saturation exposure of HCOOH; X_{Ni}, nickel surface fraction; ⊞, data points from the alloy study; ○, data point from the clean Ni(110) study.

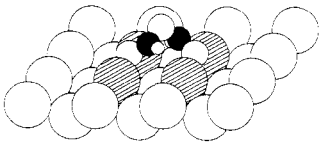

Figure 7. Schematic representation of the formic anhydride intermediate stabilized by a rectangular array of four nickel atoms on a Ni/Cu(110) alloy surface. ▨, nickel atoms; ◯, copper atoms; ○, oxygen atoms; ●, carbon atoms; ∘, hydrogen atoms.

their CO/CO thermal desorption results. In general, four CO binding states were observed on the Ni/Cu alloy surface. The highest and the lowest binding states were identified as the pure surface nickel and copper sites, respectively, whereas the two intermediate states were ascribed to the mixed Ni–Cu binding sites. The magnitudes of the CO signal from the mixed Ni–Cu binding states were as abundant as those from the pure Ni and pure Cu binding states. If surface clustering on the Ni/Cu alloy was significant, the mixed Ni–Cu binding states would be relatively negligible. The results of the present study of the formic acid decomposition on the Ni/Cu alloy also manifested this random feature. If surface clustering were significant, the CO product from the formic anhydride would not drop so markedly as the surface composition was decreased from 87% Ni to 37% Ni. In addition, if large nickel islands were formed, one would expect to observe the superposition of nickel and copper decomposition behavior, which in fact was not detected for the entire range of concentration studied. Therefore, it appears reasonable to conclude the Ni/Cu alloy surface to be a random substitutional alloy surface. Figure 6 shows a ln–ln plot of the amount of CO formed following saturation exposure of formic acid vs. nickel surface atom fraction. This plot yielded a straight line with a slope of 3.8 ± 0.2, suggesting that the CO formation required a cluster of four nickel atoms.

It is reasonable to expect the anhydride intermediate to be stabilized by a rectangular array of the four nickel atoms required as shown in Figure 7. The two CHO groups of the formic anhydride molecule were rotated 90° in opposite direction from the coplanar configuration, causing the oxygen atom of each group to sit between two nickel atoms as shown in the figure. The requirement of this "homogeneous" cluster for the stabilization of the surface anhydride controlled the relative amount of the two surface intermediates, thereby

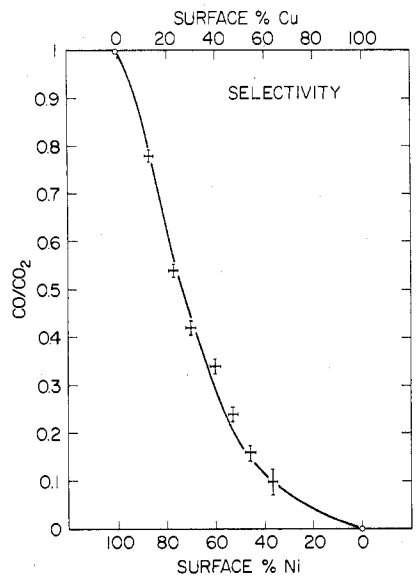

Figure 8. $CO:CO_2$ selectivity ratio as a function of surface composition: ⊣⊢, data points from the alloy study; O, data points from the clean Ni(110) and clean Cu(110) studies.

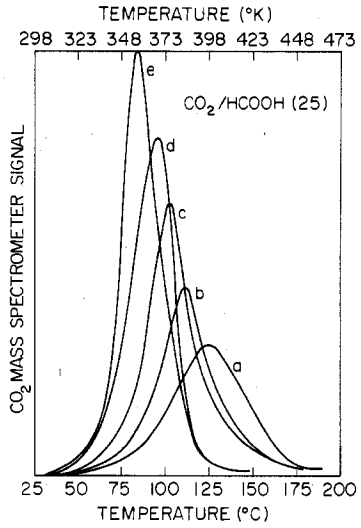

Figure 9. CO_2 product flash-desorption spectra as a function of surface composition of the alloy: curve a, 37% Ni/63% Cu; curve b, 54% Ni/46% Cu; curve c, 61% Ni/39% Cu; curve d, 68% Ni/32% Cu; curve e, 87% Ni/13% Cu. The heating rate was 12 K/s.

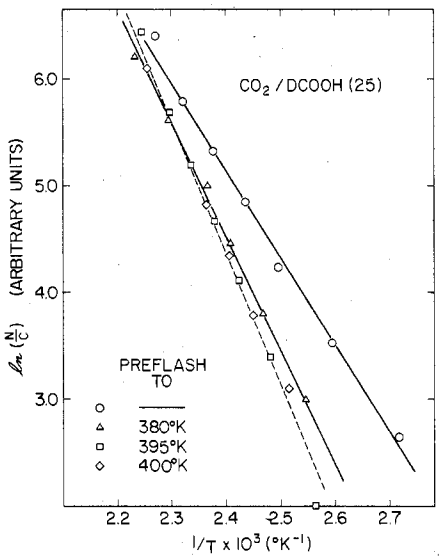

Figure 10. Plot of ln (N/C) vs. the reciprocal temperature for the series of CO_2/DCOOH "interrupted" flashes, on the alloy of 37% Ni/63% Cu.

determining the selectivity of the alloys shown in Figure 8. The $CO:CO_2$ product ratio dropped from unity as observed on clean Ni(110) surface[1-3] continuously to zero as observed on clean Cu(110) surface.[4] This change of the product ratio as a function of the alloy surface composition manifested the effect of alloying on the selectivity toward the two decomposition paths of formic acid. Furthermore, the activity of the surface nickel was retained through the stabilization of the formic anhydride intermediate by a cluster of four nickel atoms, in agreement with the localized surface electronic structure suggested by Spicer et al.[12,13]

In addition to the homogeneous cluster of four nickel atoms required to stabilize the formic anhydride intermediate, "heterogeneous" clusters apparently led to the formation of the formate intermediate (HCOO(a)). This intermediate probably existed bonded to many different types of clusters of nickel and copper atoms such as NiNi, NiCu, NiCuNi, CuNiCu, etc., each with slightly different bonding characteristics, yielding the observed CO_2 product spectrum as a superposition of all of these possible situations. When the surface composition changed, the population of each of these "heterogeneous" clusters changed, affecting the subsequent CO_2 product spectrum. Since HCOO(a) decomposed on a clean Cu(110) surface at a temperature much higher than on the alloy surfaces, it was reasonable to believe that a heterogeneous cluster consisting of relatively more copper atoms had a slightly higher activation energy giving rise to the CO_2 peak shift to higher temperatures with increasing copper concentration as shown in Figure 9. The absence of the higher temperature CO_2 states corresponding to Cu(110) on the nickel-rich surfaces also suggested that the HCOO intermediate bonded to more than one copper atom.

The activation energy for CO_2 formation was measured by varying the heating rate.[25] Since the rate of CO_2 formation was governed by the decomposition of both surface intermediates, the observed CO_2 product spectrum was a composite peak. The activation energy measured was an apparent or weighted-average value. The exact weighting was not known, and it was unlikely that it could be resolved because too many variables were involved. However, adsorbed formate was the predominant surface intermediate observed on the 37% Ni/63% Cu alloy surface. Therefore, the measured activation energy value of 26 kcal/mol on this alloy surface provided a good estimate of the energy for the decomposition of the formate on the alloy. Similarly, the measured value of 24.7 kcal/mol on the 87% Ni/13% Cu alloy surface represented the activation energy required for the decomposition of the formic anhydride on the alloy since this was the predominant surface intermediate observed. This value, together with the estimated 2 kcal/mol change from the shift of the Co(α) peak, suggested that the activation energy for the decomposition of the formic anhydride intermediate varied from 25 to 27 kcal/mol as the copper surface concentration was increased.

The results of "interrupted" flashes showed that as the alloy sample with a surface composition of 37% Ni/63% Cu was preflashed to above 360 K, both the CO_2/DCOOH and the D_2/DCOOH peaks shifted to a higher temperature. With an assumption of a first-order process, a plot of ln (N/C) vs. the reciprocal temperature was used to measure the apparent activation energy of the "interrupted" CO_2 flash peak as shown in Figure 10. By means of this method, the apparent activation energy was found to increase gradually from 17 kcal/mol to a final value of 26.5 kcal/mol as the preflash temperature was increased. The results of the interrupted flashes can be ascribed to the surface site heterogeneity. The

preflash apparently resulted in the flashing off of surface intermediates with lower activation energies, revealing the characteristics of those remaining; the formic anhydride was probably flashed off first since it showed the lower activation energy for decomposition, leaving essentially the adsorbed formate. Therefore, the CO_2 "interrupted" spectrum reflected primarily the contribution due to the adsorbed formate. In turn, due to the existence of different binding states for the HCOO(a), the adsorbed formate with the lowest decomposition energy was flashed off first, eventually leaving only the one with the highest decomposition energy. The limiting value of 26.5 kcal/mol represented the highest activation energy required for the decomposition the formate on the alloy. The close agreement between this limiting value and the apparent activation energy measured on the 37% Ni/63% Cu alloy surface further supported that it was a good estimation for the decomposition of the formate on the alloy.

In conclusion, it is interesting to compare these results with the catalytic decomposition of formic acid on the carburized Ni(110) surface studied by McCarty and Madix.[26-28] In that study, adsorbed formate was found to be the predominant surface intermediate observed, and the $CO:CO_2$ product ratio was about 0.1, similar to that observed for the 37% Ni/63% Cu alloy surface. The close resemblance of the selectivity and the intermediate involved between these two surfaces suggested that the presence of surface carbidic carbon modifies surface reactivity in a fashion similar to alloying with a group 1B element. The results of the present study clearly manifested the importance of clusters in the selectivity and activity for the formic acid decomposition on the Ni/Cu alloy. The present study highlights the fact that the ligand effects can be secondary to the cluster requirement in the surface reactivity of alloys.

Acknowledgment. The authors gratefully acknowledge the support of this work by the National Science Foundation, Grant NSF-DMR 74-22230, through the Center for Materials Research at Stanford. The authors also thank Dr. T. Dickinson of the Physics Department of Washington State University for his contributions during the initial stages of the work.

Registry No. Cu/Ni, 11101-28-3; formic acid, 64-18-6; formic anhydride, 1558-67-4.

References and Notes

(1) J. Falconer and R. J. Madix, *Surf. Sci.*, **46**, 473 (1974).
(2) J. Falconer, J. McCarty, and R. J. Madix, *Surf. Sci.*, **42**, 329 (1974).
(3) J. Falconer, Ph.D Dissertation, Stanford University, 1974.
(4) D. H. S. Ying and R. J. Madix, to be submitted for publication.
(5) H. Verbeck and W. M. H. Sachtler, *J. Catal.*, **42**, 257 (1976).
(6) V. Ponec, *Catal. Rev.-Sci. Eng.*, **11** (1), 1 (1975).
(7) V. Ponec and W. M. H. Sachtler, *Catal., Proc. Int. Congr., 5th*, 645 (1973).
(8) J. H. Sinfelt, J. L. Carter, and D. J. C. Yates, *J. Catal.*, **24**, 283 (1972).
(9) J. S. Campbell and P. H. Emmett, *J. Catal.*, **7**, 252 (1967).
(10) D. A. Dowden and P. W. Reynolds, *Faraday Discuss. Chem. Soc.*, **No. 8**, 184 (1950).
(11) P. W. Reynolds, *J. Chem. Soc.*, 265 (1950).
(12) K. Y. Yu, Ph.D. Dissertation, Stanford University, 1976.
(13) K. Y. Yu, C. R. Helms, and W. E. Spicer, *Solid State Commun.*, **18**, 1365 (1976).
(14) F. L. Williams, Ph.D. Dissertation, Stanford University, 1972.
(15) F. L. Williams and P. Nason, *Surf. Sci.*, **45**, 377 (1974).
(16) J. J. Burton and E. S. Macklin, submitted for publication in *Phys. Rev. Lett.*
(17) J. C. Tracy in "Auger Electron Spectroscopy for Surface Analysis".
(18) S. C. Moss, *Phys. Rev. Lett.*, **23**, 38 (1969).
(19) D. R. Buytymowicz, J. R. Manning, and M. E. Read, *J. Phys. Chem. Ref. Data*, **2**, 643 (1973).
(20) K. Y. Yu, D. T. Ling, and W. E. Spicer, *J. Catal.*, **44**, 373 (1976).
(21) K. Y. Yu, D. T. Ling, and W. E. Spicer, *Solid State Commun.*, **20**, 751 (1976).
(22) J. McCarty, J. Falconer, and R. J. Madix, *J. Catal.*, **30**, 235 (1973).
(23) J. Falconer and R. J. Madix, *Surf. Sci.*, **48**, 393 (1975).
(24) D. H. S. Ying and R. J. Madix, unpublished data.
(25) J. Falconer and R. J. Madix, *Surf. Sci.*, **48**, 393 (1975).
(26) J. McCarty and R. J. Madix, *J. Catal.*, **38**, 402 (1975).
(27) J. McCarty, Ph.D. Dissertation, Stanford University, 1974.
(28) J. McCarty, J. Falconer, and R. J. Madix, *J. Catal.*, **31**, 316 (1973).

Contribution from the Department of Chemistry, University of Georgia, Athens, Georgia 30602, and the Office of Naval Research, Arlington, Virginia 22217

Adducts of Arsenic(III) Halides and Arylarsenic(III) Halides with Thioureas

DANIEL J. WILLIAMS[1a] and KENNETH J. WYNNE*[1b]

Received March 16, 1977

A series of arsenic trihalide and arylarsenic dihalide adducts with thioureas have been prepared. New compounds which have been characterized include AsX_3B [X = Cl, Br; B = tmtu (1,1,3,3-tetramethyl-2-thiourea), dmit (1,3-dimethyl-2(3*H*)-imidazolethione)] and $ArAsX_2tmtu$ [Ar = C_6H_5, 4-$CH_3C_6H_4$, X = Cl, Br, I; Ar = 4-$CH_3OC_6H_4$, 4-ClC_6H_4, 4-$O_2NC_6H_4$, X = Cl]. These adducts are thermally stable at ambient temperature but decompose on exposure to atmospheric moisture at varying rates (Cl ≫ Br; AsX_3B > $ArAsX_2tmtu$). Adducts were characterized by infrared, Raman, and proton nuclear magnetic resonance spectroscopy. The adducts were found to be molecularly dissociated in solution to varying degrees; the order of acceptor ability toward thioureas is $AsBr_3$ > $AsCl_3$; $ArAsI_2$, $ArAsBr_2$ > $ArAsCl_2$. Assignments for solid-state Raman and infrared spectra for the adducts are reported. Trigonal-bipyramidal structures are proposed for the adducts based on vibrational spectra. Secondary bonding leading to the formation of loosely joined dimeric molecules may occur as found by x-ray crystallography for $AsCl_3$dmit.

The acceptor properties of group 5A trihalides and organic derivatives RMX_2 and R_2MX are well established in the literature.[2-12] While the synthesis of numerous adducts has been reported, there have been surprisingly few attempts to determine the structures of these compounds. The overall lack of structural information is due in part to the fact that many of these adducts were made in the early part of this century prior to the advent of modern instrumental techniques.[4-8] Structures which are known via single-crystal x-ray analysis include $AsCl_3NMe_3$[9] (Me = methyl), $SbCl_3NH_2C_6H_5$,[10] $SbCl_3(Ph_3AsO)_2$[2] (Ph = phenyl), and $Me_2AsCl(tu)_2$[11,12] (tu = thiourea). Vibrational spectra for $AsCl_3NMe_3$ and $SbCl_3NH_2C_6H_5$ have been used in conjunction with the above structural studies for spectral interpretation of analogous compounds such as PCl_3NMe_3 and PBr_3NMe_3.[13] For the most part, however, vibrational data have been used primarily to demonstrate coordination as indicated by shifts in known bands. The lowering of the P=O stretching mode in tri-

0020-1669/78/1317-1108$01.00/0